Mechanochemical Synthesis of Corannulene-Based Curved Nanographenes

Gábor Báti,[a] Dániel Csókás,[b] Teoh Yong,[a] Si Man Tam,[a] Raymond R. S. Shi,[a] Richard D. Webster,[a] Imre Pápai,[b] Felipe Garcia,*[a] and Mihaiela C. Stuparu*[a]

[a] Dr. G. Báti, Y. Teoh, S. M. Tam, S. R. R. Shi, Prof. R. D. Webster, Prof. F. Garcia, Prof. M. C. Stuparu
Division of Chemistry and Biological Chemistry
School of Physical and Mathematical Sciences, Nanyang Technological University Singapore
21 Nanyang Link, 637371 Singapore (Singapore)
E-mail: fgarcia@ntu.edu.sg, mstuparu@ntu.edu.sg

[b] Dr. D. Csókás, Prof. I. Pápai
Institute of Organic Chemistry
Research Center for Natural Sciences
Magyar tudósok körútja 2, H-1117 Budapest, Hungary

Supporting information for this article is given via a link at the end of the document.

Abstract: Herein we show that corannulene-based strained π-surfaces can be obtained through the use of mechanochemical Suzuki and Scholl reactions. Besides being solvent-free, the mechanochemical synthesis is high-yielding, fast, and scalable. Therefore, gram-scale preparation can be carried out in a facile and sustainable manner. The synthesized nanographene structure carries positive (bowl-like) and negative (saddle-like) Gaussian curvatures and adopts an overall quasi-monkey saddle-type of geometry. In terms of properties, the non-planar surface exhibits a high electron affinity that was measured by cyclic voltammetry, with electrolysis and *in situ* UV-vis spectroscopy experiments indicating that the one-electron reduced state displays a long lifetime in solution. Overall, these results indicate the future potential of mechanochemistry in accessing synthetically challenging and functional curved π-systems.

Introduction

Curvature of π-surfaces endows nanographenes with unusual structure and properties.[1-4] Such curvature can be induced through the incorporation of steric constraints or non-hexagonal rings into the molecular structure.[4] The solution-phase synthesis of these materials often requires long reaction times, results in low overall yields, and produces large amounts of chemical wastes typically in the form of organic solvents. These attributes do not facilitate practical access to large material quantities in a sustainable manner. This creates a need for the development of alternative pathways to meet the future demands on the synthesis of curved π-materials.

Recently, mechanochemistry has emerged as a powerful synthetic tool in the preparation of organic, inorganic, and polymeric materials.[5] In this approach, mechanical energy through grinding or milling action is used to facilitate a chemical reaction.[6] Such reactions are known to be solvent-free, high yielding, fast, and scalable.[7] Finally, unlike solution-phase synthesis in which solubility of the reactants and the products often determines the fate of a reaction, mechanochemical reactions remain undeterred by such parameters.[8] These attributes bode well for the preparation of strained π-systems[9] and serves as a motivation for the present work.[10]

To evaluate the feasibility of the aforementioned notion, we chose to prepare corannulene-phenanthrene hybrid **1**, a novel $C_{44}H_{22}$ structure (Scheme 1). In their seminal studies involving tetrabromocorannulene,[11] Sygula and Rabideau reported that such a hybrid structure could not be prepared through oxidative coupling or photochemical annulation methods in solution.[12] They concluded that the curvature of the structure hindered its formation. Interestingly, the authors mentioned that flash vacuum pyrolysis - a gas-phase synthetic technique - was being explored. This technique, as established by Scott and coworkers, is the most powerful method to induce molecular curvature as seen in the landmark chemical synthesis of fullerene C_{60}.[13] However, **1** remains unknown to date. Therefore, it presents an excellent target to evaluate the credentials of mechanochemistry as an alternative synthetic tool to conventional solution- and gas-phase chemistries.

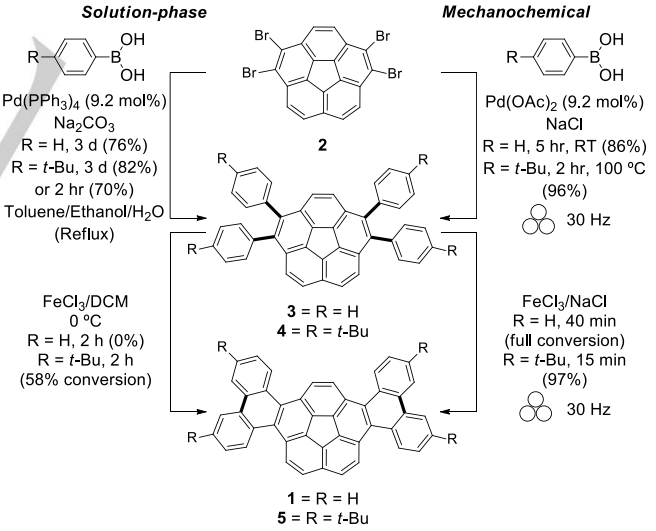

Scheme 1. Synthesis of curved π-systems.

Results and Discussion

The synthesis of **1** requires a two-step process (Scheme 1). In the first step, tetrabromocorannulene (**2**), which can now be accessed on a kilogram scale,[14] is subjected to a Suzuki reaction with phenyl boronic acid to install the aromatic units on the adjacent carbon atoms, thus affording **3**. A subsequent *o*-terphenyl to triphenylene cyclization through Scholl reaction would then lead to the target structure **1**.

To understand the mechanochemical Suzuki reaction,[15] various reaction parameters were examined in a mixer mill (electronic supporting information-I (ESI-I) Table S1). In terms of catalyst, $Pd(OAc)_2$ (9.2 mol%) performed better than $Pd(PPh_3)_4$.[16] Sodium chloride was a better bulking agent than silica and potassium carbonate. The boronic acid-based coupling partner provided the best results when used in an 8-fold excess. Larger excess, however, led to a decrease in the isolated yields. A ligand was not required for the cross-coupling reaction. The reaction performed best in the presence of a single 15 mm stainless steel ball in a 30 mL stainless steel jar and a 5 h reaction time. Longer reaction times did not improve the yields. However, an oxygen-free atmosphere was found to be necessary for the optimum reactivity. The optimized reaction could be reproduced multiple times (>10) and consistently provided **3** with isolated yields of >85%.

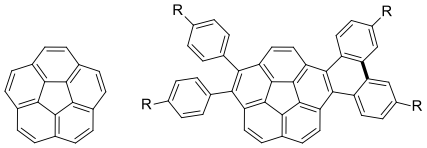

6 **7** = R = *t*-Bu

Figure 1. Chemical structure of corannulene **6** and compound **7**.

The next step was to study the Scholl reaction using $FeCl_3$.[17-19] Initially, 1 equivalent (equiv.) of the oxidant per abstracted H atom was used. This led to the formation of a mixture of singly and doubly benzannulated products in low yields. The amount of the oxidant was then increased to 2 and 3 equiv./H atom and led to similar formation of a mixture of products. A further increase to 4 equiv./per H atom led to complete conversion of **3** to **1** in a 40 minutes reaction time as judged by the examination of the crude reaction mixture with the help of ^{1}H-NMR.

Whilst these results were very encouraging, **1** exhibited limited solubility in a range of organic solvents. Therefore, a tertiary-butyl (*t*-Bu) group was installed onto the molecular scaffold (**4**) to enhance solubility and aid purification, characterization, and crystallization attempts. Interestingly, it was observed that attaching heat-pads to the mixer mill could shorten the Suzuki reaction time to 2 hours at a temperature of 100 °C (product yield = 86%) (ESI-I Table S2 and Figure S1). Furthermore, purity of the starting material was also found to be important. For instance, under optimized condition, use of recrystallized **2** led to a 10% enhancement in the isolated yield. The Scholl reaction also proceeds well regardless of the jar and milling ball material (ESI-I Figure S2) and leads to the formation of **5** in 97% isolated yield in a 15 minutes reaction time. The reactions could be easily scaled up to a 1-gram scale (ESI-I Figure S3-S4) either by use of a planetary mill or by multiple reiterations of the small-scale reaction. Due to high yields and absence of side products as can be seen in the crude NMR (ESI-I Figure S2), the purifications are simple and a complete gram-scale synthesis can be achieved within two days.

A solution-phase synthesis of **3** is described by Sygula and Rabideau in the aforementioned study on **1**.[12] In a reaction time of 24 hours, **3** was produced in a 66% yield through use of $Pd(PPh_3)_4$ as a catalyst. We prolonged the reaction time to 3 days with a 10% enhancement in the isolated yield (76%). In the case of **4**, a 3 day reaction produced a better yield of 82% perhaps due to a better solubility of **4** as compared to **3**. In this case, for the sake of a better comparison to mechanochemical reaction, a 2 hour reaction was also carried out. The short reaction time led to a decrease in the isolated yield (70%). It must be mentioned that application of related Suzuki protocols on corannulene (**6**, Figure 1) scaffolds or a systematic optimization of the reaction may provide better yields and faster reaction times.[20]

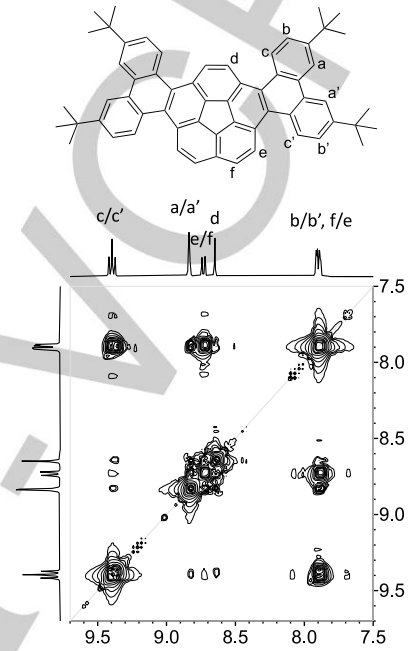

Figure 2. Signal assignments through COSY ^{1}H-NMR data of **5** in deuterated chloroform at room temperature.

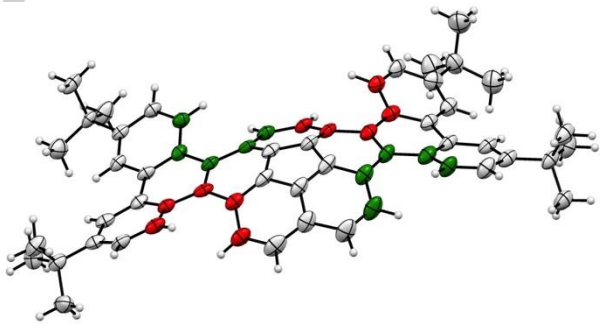

Figure 3. ORTEP representation of a single molecule of **5** with 50% probability of ellipsoids. The *P* and *M* [4]helicenes are shown with red and green colors, respectively.

To examine the solution-phase Scholl reaction, typical protocols involving $FeCl_3$ and nitromethane or DDQ and methanesulfonic/triflic acids in dichloromethane were employed. However, based on crude NMR, no conversion of **3** to **1** was observed in line with the observations of Sygula and Rabideau.[12] Due to a limited solubility of **1**, the focus was turned onto **5**. This study indicated that the solution phase reactions produce a mixture of compounds including the starting material **4**, mono-coupled product **7**, and the target compound **5**. The most successful reaction in this regard is the treatment with

$FeCl_3$ for 2 hours at 0 °C which produces 58% of **5** based on crude ^{1}H-NMR (ESI-I Figure S5). However, a column chromatography separation is difficult presumably due to a very close molar mass and polarity of the three compounds. Preparative thin layer chromatography was also found to be unsuccessful in this regard albeit allowing access to **7** in a 20% isolated yield.

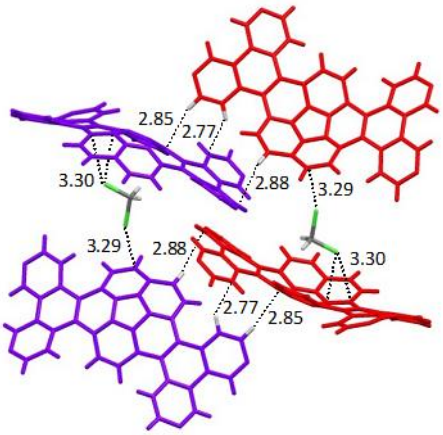

Figure 4. Molecular packing in single crystal X-ray structure of **5**. The *t*-butyl groups have been omitted for clarity.

The structure of **5** was determined with the help of NMR studies in solution and X-ray crystallography. The aromatic proton resonances could be assigned with the help of cross-peaks in 2D COSY ^{1}H-NMR data (Figure 2). In X-ray crystallography studies (Figure 3-5), **5** crystallises as a dichloromethane solvate in a 1:1 ratio in the $P2_1/c$ space group.[21] The solvate forms a wavy chain displaying both single (mean 3.29 Å) and bifurcated (mean 3.30 Å) C-Cl π-aryl interactions. While the solute (**5**) forms two interlocked undulating chains with central aromatic bowls pointing in opposite directions and multiple short C-H π-aryl interactions (2.77, 2.85, 2.88 Å) connecting the strands.

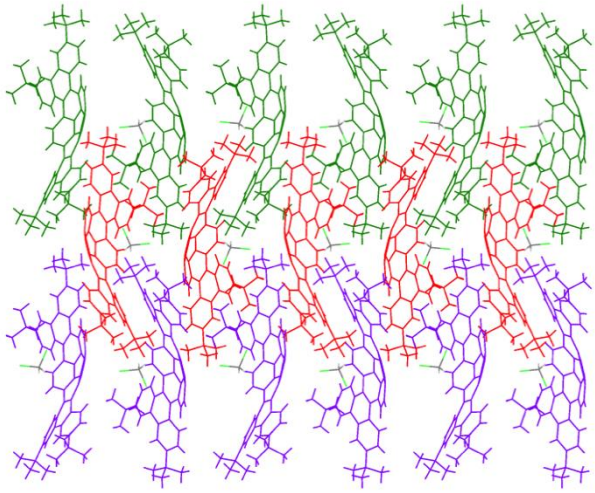

Figure 5. Perspective view along crystallographic *a*-axis showing interlocked arrangement of three molecular chains (shown with the help of different colors) in the crystal lattice of **5**.

The crystal structure also provides an opportunity to examine curvature of the π-surface in **5.** For instance, the torsional angles undergo large and drastic variations on moving from the center to the peripheral positions on the molecular framework (ESI-I Figure S6). The maximum distortion can be found adjacent to the central five-membered ring. This tension eases steadily towards the proximal rings. The incorporation of the peripheral phenanthrene wings leads to a slight decrease in the central bowl-depth (0.85 Å) as compared to pristine corannulene (0.87 Å). The wings display a saddle shape with negative curvatures[22] while the corannulene core displays a positive Guassian curvature. Overall, the molecule is comprised of waves of warped and twisted aromatic ribbons with gradual changes in the clockwise and anticlockwise dihedral angles to form a quasi-monkey saddle type of topology (ESI-I Figures S7-S9, an interactive plot is provided as ESI-II).[23]

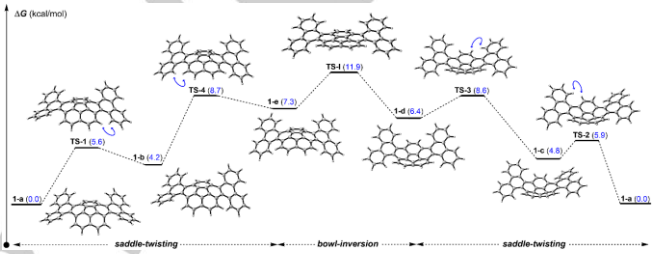

Figure 6. Free energy profile of a computationally identified bowl-inversion process for **1**. Relative stabilities are given in parenthesis (in kcal/mol) with respect to **1-a** conformer. The blue arrows indicate where saddle-twisting occurs. For additional conformers and transition states, see ESI-I.

The geometry of the molecule was well reproduced by DFT computations at the ωB97X-D/def2SVP level of theory.[24] Among six computationally identified conformational isomers (ESI-I Figure S10), the most stable conformer was calculated to be **1-a**, which corresponds to the geometry found by single-crystal X-ray crystallography.

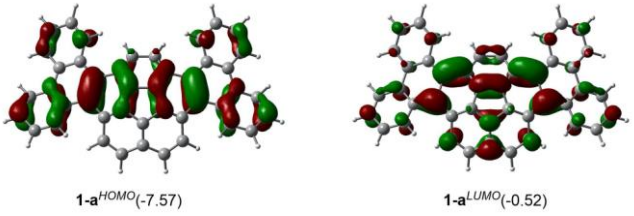

Figure 7. Frontier molecular orbitals of the curved surface in the quasi-monkey saddle structure (isovalue = 0.03). Orbital energies calculated at the ωB97X-D/Def2TZVPP level are given in parenthesis (in eV). For computations, the *t*-Bu groups were excluded from the molecular structure for simplicity reasons.

Computations also allowed for examining the dynamic nature of the molecule through bowl-inversion and saddle-twisting process. A fully planar transition state (**TS$_{hyp}$**), in which the entire π-system is in a plane, could not be computationally identified as a viable route to structural inversion (ESI-I Figure S11). However, we found alternative pathways for the molecular inversion to occur under ambient conditions. The free energy profile of such a feasible interconversion is presented in Figure 6 (for further possible ways of interconversion and related transition states

see ESI-I Figure S12-S13). The highest lying transition state **TS-I** is predicted to be 11.9 kcal/mol above **1-a** connecting conformers **1-e** and **1-d** via a small barrier, which indicates that the bowl-inversion is feasible at ambient temperature. For this to occur, the π-system is required to adopt a conformation of **1-e** or **1-d**. This means that one of the saddles is required to switch to the twisted arrangement as the first step. The lowest transition state of this conformational change, **TS-1** connecting **1-a** with **1-b**, was found to be 5.6 kcal/mol. **TS-2** corresponding to the interconversion between **1-a** and **1-c** is slightly higher in energy (5.9 kcal/mol). The second saddle can then switch to the twisted arrangement with ease via **TS-4** (8.7 kcal/mol) from **1-b** or **TS-3** (8.6 kcal/mol) from **1-c**. This indicates that the interconversion of the conformers is rapid, ultimately allowing for a molecular flipping process to take place and the molecule to invert.

The frontier molecular orbitals of the most stable form of **1** are depicted in Figure 7. The highest occupied molecular orbital (HOMO) is found to be localized on the saddle and the lowest occupied molecular orbital (LUMO) on the bowl region of the curved surface.

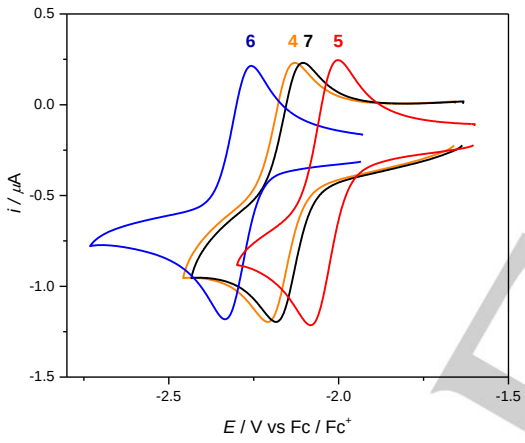

Figure 8. Cyclic voltammograms showing reduction processes of 1 mM corannulene **6** (blue) and compounds **4** (orange), **7** (black), and **5** (red) in DMF containing 0.1 M *n*-Bu_4NPF_6.

Finally, electrochemical properties were studied with the help of cyclic voltammetry and square-wave voltammetry experiments in dimethylformamide (Figure 8 and ESI-I Figure S14).[25] In comparison to corannulene **6** (E_{red}^1 = -2.30 V), which only represents the bowl, **4** showed an increase in the electron affinity with an anodic shift of 0.09 V (E_{red}^1 = -2.21 V). Introduction of the first saddle leads to a further enhancement of the electron affinity by 0.16 V in molecule **7** (E_{red}^1 = -2.14 V).[26] Incorporation of the second saddle into the molecule shifts the first reduction potential further towards the anode by 0.22 V in **5** (E_{red}^1 = -2.08 V). More importantly, however, the stability of the reduced species was found to be remarkable. Figure 9 shows the UV-vis spectra obtained during the one-electron reduction of **5**. The neutral form of **5** displayed several UV-vis absorbance bands below 370 nm, whereas the reduced form exhibited several additional low intensity absorbance bands between 450 to 700 nm. The additional higher wavelength (low energy) bands in the radical anion are expected for an open shell molecule since there is a narrowing of the energy gap between the singly occupied HOMO and the LUMO, compared to the electronic transitions that occur from the diamagnetic ground state of compound **5**. Similar bands are seen in the one-electron reduced form of C_{60} that extends into the NIR region.[27] The electrolysis process was carried out for one hour in the forward direction. The UV-vis spectra of the neutral form of **5** could be regenerated in its entirety when an oxidising potential was applied to the solution that was initially reduced, thus indicating full reversibility of the reduction process (ESI-I Figure S15). To our knowledge, such an exhaustive procedure to establish reversibility of the electron accepting properties has never been demonstrated in any of the known non-planar nanographenes.

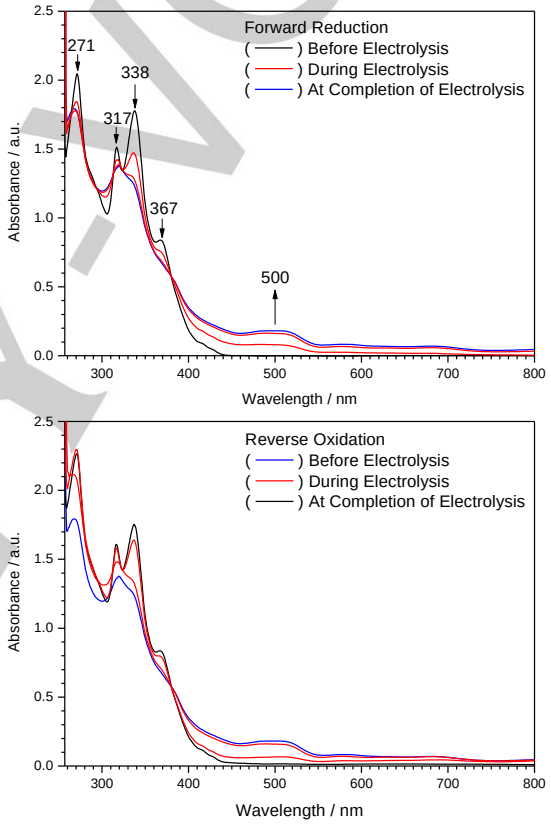

Figure 9. *In-situ* UV-vis spectra of 0.4 mM compound **5** and its one-electron reduced form obtained in an optically semi-transparent thin layer electrochemical (OSTLE) cell in DMF containing 0.2 M Bu_4NPF_6 at -25 °C. (*top*) Before and during the one-electron bulk reduction of compound **5**. (*bottom*) Before electrolysis of compound **5** and after reduction of the compound then reoxidised back to its neutral form.

Conclusion

In summary, mechanochemistry offers a viable alternative to solution and gas-phase synthesis of curved π-systems. As exemplified by corannulene-phenanthrene hybrid, the practicality of the solvent-free synthesis allows for readily available precursors to be assembled into complex non-planar nanographene structures with remarkable electronic properties within a two-day period. The synthesis can be carried out on a gram-scale and shows immense potential of mechanochemical

reactions in accessing synthetically challenging curved nanographenes that cannot be accessed via conventional chemistries.

Acknowledgements

Financial support from the Ministry of Education Singapore under the AcRF Tier 1 (2019-T1-002-066) (RG106/19) (2018-T1-001-176) (RG18/18); Agency for Science, Technology and Research (A*STAR)-AME IRG A1883c0006 and A1783c0003; and NTU (04INS000171C230, M4080552) is gratefully acknowledged. Computer facilities provided by NIIF HPC Hungary (project 85708 kataproc) are also acknowledged. We thank Dr. Zsolt Szabó for visualizing the ideal- and quasi-monkey saddle surfaces. Dr. Yongxin Li's efforts in conducting X-ray crystallographic measurements is highly appreciated. We also thank Ms. Dzeneta Halilovic for help with MALDI-TOF and optical measurements. Finally, Mr. Tony Gan Eng Swee and his 'Making and Thinkering' team is thanked for creating the heat pads for the mixer mills.

Keywords: sustainable chemistry • mechanochemistry • ball milling • fused-ring systems • solventless reactions

[1] For an excellent discussion on molecular curvature, see: M. Rickhaus, M. Mayor, M. Juríček, *Chem. Soc. Rev.* **2017**, *46*, 1643-1660.

[2] K. K. Baldridge, J. S. Siegel, *Angew. Chem. Int. Ed.* **2013**, *52*, 5436-5438; *Angew. Chem.* **2013**, *125*, 5546-5548.

[3] F. Banhart, J. Koakoski, A. V. Krasheninnikov, *ACS Nano* **2011**, *5*, 26-41.

[4] For review of this area, see: a) L. T. Scott, *Pure Appl. Chem.* **1996**, *68*, 291-300; b) V. M. Tsefrikas, L. T. Scott, *Chem. Rev.* **2006**, *106*, 4868-4884; c) Y.-T. Wu, J. S. Siegel, *Chem. Rev.* **2006**, *106*, 4843-4867; d) D. Kuck, *Chem. Rev.* **2006**, *106*, 4885-4925; e) A. Sygula, *Eur. J. Org. Chem.* **2011**, *2011*, 1611-1625; f) M. Stępień, *Synlett* **2013**, *24*, 1316-1321; g) Q. Miao, *Chem. Rec.* **2015**, *15*, 1156-1159; h) M. Ball, Y. Zhong, Y. Wu, C. Schenck, F. Ng, M. Steigerwald, S. Xiao, C. Nuckolls, *Acc. Chem. Res.* **2015**, *48*, 267-276; i) Y. Segawa, H. Ito, K. Itami, *Nat. Rev. Mat.* **2016**, *1*, 15002; j) Y. Segawa, A. Yagi, K. Matsui, K. Itami, *Angew. Chem. Int. Ed.* **2016**, *55*, 5136-5158; *Angew. Chem.* **2016**, *128*, 5222-5245; k) L. T. Scott, *Pure Appl. Chem.* **2017**, *89*, 809-820; l) I. R. Márquez, S. Castro-Fernández, A. Millán, A. G. Campaña, *Chem. Commun.* **2018**, *54*, 6705-6718; m) S. H. Pun, Q. Miao, *Acc. Chem. Res.* **2018**, *51*, 1630-1642; n) E. Nestoros, M. C. Stuparu, *Chem. Commun.* **2018**, *54*, 6503-6519; o) M. A. Majewski, M. Stępień, *Angew. Chem. Int. Ed.* **2019**, *58*, 86-116; *Angew. Chem.* **2019**, *131*, 90-122; p) E. M. Muzammil, D. Halilovic, M. C. Stuparu, *Commun. Chem.* **2019**, *2*, 1-13.

[5] For review articles, see: a) B. Rodríguez, A. Bruckmann, T. Rantanen, C. Bolm, *Adv. Synth. Catal.* **2007**, *349*, 2213-2233; b) A. Bruckmann, A. Krebs, C. Bolm, *Green Chem.* **2008**, *10*, 1131-1141; c) S. L. James, C. J. Adams, C. Bolm, D. Braga, P. Collier, T. Friščić, F. Grepioni, K. D. M. Harris, G. Hyett, W. Jones, A. Krebs, J. Mack, L. Maini, A. G. Orpen, I. P. Parkin, W. C. Shearouse, J. W. Steed, D. C. Waddell, *Chem. Soc. Rev.* **2012**, *41*, 413-447; d) K. Ralphs, C. Hardacre, S. L. James, *Chem. Soc. Rev.* **2013**, *42*, 7701; e) G.-W. Wang, *Chem. Soc. Rev.* **2013**, *42*, 7668-7700; f) J. G. Hernández, C. Bolm, *J. Org. Chem.* **2017**, *82*, 4007-4019; g) J. L. Howard, Y. Sagatov, L. Repusseau, C. Schotten, D. L. Browne, *Green Chem.* **2017**, *41*, 413; h) A. A. Gečiauskaitė, F. García, *Beilstein J. Org. Chem.* **2017**, *13*, 2068–2077; i) J-L. Do, T. Friščić, *ACS Cent. Sci.* **2017**, *3*, 13-19; j) J. L. Howard, Q. Cao, D. L. Browne, *Chem. Sci.* **2018**, *9*, 3080-3094; k) J. Andersen, J. Mack, *Green Chem.* **2018**, *20*, 1435-1443; l) J. L. Howard, M. C. Brand, D. L. Browne, *Angew. Chem. Int. Ed.* **2018**, *57*, 16104-16108; *Angew. Chem.* **2018**, *130*, 16336-16340; m) Q. Cao, J. L. Howard, E. Wheatley, D. L. Browne, *Angew. Chem. Int. Ed.* **2018**, *57*, 11339-11343; *Angew. Chem.* **2018**, *130*, 11509-11513; n) Q. Cao, W. I. Nicholson, A. C. Jones, D. L. Browne, *Org. Biomol. Chem.* **2019**, *17*, 1722-1726; o) Q. Cao, R. T. Stark, I. A. Fallis, D. L. Browne, *ChemSusChem* **2019**, *12*, 2554-2557; p) D. Tan and F. Garcia, *Chem. Soc. Rev.* **2019**, *48*, 2274-2292; q) T. Friščić, C. Mottillo, H. M. Titi, *Angew. Chem. Int. Ed.* **2020**, *59*, 1018-1029; *Angew. Chem.* **2020**, *132*, 1030-1041. r) W. Pickhardt, S. Grätz, L. Borchardt, *Chem. Eur. J.* **2020**, DOI:10.1002/chem.202001177.

[6] Reactions between solids are typical, however, the method can also be extended to gaseous reactants. For an excellent review of this emerging area of research, see: J. G. Hernández, C. Bolm, *Angew. Chem. Int. Ed.* **2019**, *58*, 3285-3299; *Angew. Chem.* **2019**, *131*, 3320-3335.

[7] For an embodiment of these in a recent work, see: Q. Cao, D. E. Crawford, C. Shi, S. L. James, *Angew. Chem. Int. Ed.* **2020**, *59*, 4478-4483; *Angew. Chem.* **2020**, *132*, 4508-4513.

[8] This can be seen in the preparation of porous organic and crosslinked polymers: a) E. Troschke, S. Grätz, T. Lübken, L. Borchardt, *Angew. Chem. Int. Ed.* **2017,** *56,* 6859-6863; *Angew. Chem.* **2017**, *129*, 6963-6967; b) S. Grätz, S. Zink, H. Kraffczyk, M. Rose, L. Borchardt, *Beilstein J. Org. Chem.* **2019,** *15,* 1154-1161; c) X. Zhu, C. Tian, T. Jin, K. L. Browning, R. L. Sacci, G. M. Veith, S. Dai, *ACS Macro Lett.* **2017**, 6, 1056-1059.

[9] O. Papaianina, V. A. Akhmetov, A. A. Goryunkov, F. Hampel, F. W. Heinemann, K. Y. Amsharov, *Angew. Chem. Int. Ed.* **2017**, *129*, 4912-4916; *Angew. Chem. Int. Ed.* **2017**, *56*, 4834-4838.

[10] For planar π-conjugated systems and polycyclic aromatic hydrocarbon preparation, see: a) J. B. Ravnsbæk, T. M. Swager, *ACS Macro Lett.* **2014,** *3,* 305–309; b) R. A. Haley, A. R. Zellner, J. A. Krause, H. Guan, J. Mack, *ACS Sustainable Chem. Eng.* **2016**, *4*, 2464-2469; c) Y. Zhao, S. V. Rocha, T. M. Swager, *J. Am. Chem. Soc.* **2016**, *138*, 13834-13837; d) C. Wang, M. Hill, B. Theard, J. Mack, *RSC Adv.* **2019**, *9*, 27888-27891; e) K. J. Ardila-Fierro, C. Bolm, J. G. Hernández, *Angew. Chem. Int. Ed.* **2019**, *58*, 12945-12949; *Angew. Chem.* **2019**, *131*, 13079-13083.

[11] A. Sygula, P. W. Rabideau, *J. Am. Chem. Soc.* **2000**, *122*, 6323-6324.

[12] a) G. Xu, A. Sygula, Z. Marcinow, P. W. Rabideau, *Tetrahedron Lett.* **2000**, *41*, 9931-9934; b) A. Sygula, G. Xu, Z. Marcinow, P. W. Rabideau, *Tetrahedron* **2001**, *57*, 3637-3644.

[13] a) M. M. Boorum, Y. V. Vasil'ev, T. Drewello, L. T. Scott, *Science*, **2001**, *294*, 828; b) L. T. Scott, M. M. Boorum, B. J. McMahon, S. Hagen, J. Mack, J. Blank, H. Wegner, A. de Meijere, *Science*, **2002**, *295*, 1500; c) L. T. Scott, *Angew. Chem. Int. Ed.* **2004**, *43*, 4994-5007; c) L. T. Scott, *Angew. Chem. Int. Ed.* **2004**, *43*, 4994-5007; *Angew. Chem.* **2004**, *116*, 5102-5116.

[14] A. M. Butterfield, B. Gilomen, J. S. Siegel, *Org. Process Res. Dev.* **2012**, *16*, 664-676.

[15] a) S. Grätz, B. Wolfrum, L. Borchardt, *Green Chem.* **2017**, *19*, 2973-2979; b) C. G. Vogt, S. Grätz, S. Lukin, I. Halasz, M. Etter, J. D. Evans, L. Borchardt, *Angew. Chem. Int. Ed.* **2019**, *58*, 18942-18947; *Angew. Chem.* **2019**, *131*, 19118-19123.

[16] For palladium-catalyzed reactions in mechanochemistry, see: a) D. A. Fulmer, W. C. Shearouse, S. T. Medonza, J. Mack, *Green. Chem.* **2009**, *11*, 1821-1825; b) L. Chen, B. E. Lemma, J. S. Rich, J. Mack, *Green. Chem.* **2014**, *16*, 1101-1103.

[17] For review of iron(III) chloride in oxidative coupling reactions, see: A. A. O. Sarhan, C. Bolm, *Chem. Soc. Rev.* **2009**, *38*, 2730-2744.

[18] a) M. O. Rasmussen, O. Axelsson, D, Tanner, *Syn. Commun.* **1997**, *27*, 4027-4030; b) S. Grätz, D. Beyer, V. Tkachova, S. Hellmann, R. Berger, X. Feng, L. Borchardt, *Chem. Commun.* **2018**, *54*, 5307-5310; c) S. Grätz, M. Oltermann, E. Troschke, S. Paasch, S. Krause, E. Brunner, L. Borchardt, *J. Mater. Chem. A*, **2018**, *6*, 21901-21905; d) X. Zhu, Y. Hua, C. Tian, C. W. Abney, P. Zhang, T. Jin, G. Liu, K. L. Browning, R. L. Sacci, G. M. Veith, H.-C. Zhou, W. Jin, S. Dai, *Angew. Chem. Int. Ed.* **2018,** *57,* 2816-2821; *Angew. Chem.* **2018**, *130*, 2866-2871.

[19] For a recent report on $FeCl_3$-free mechanochemical cyclodehydrogenation mediated by a copper surface, see: S. Graẗz, M.

Oltermann, C. G.Vogt, L. Borchardt, *ACS Sustainable Chem. Eng.* **2020**, *8*, 7569-7573.

[20] For Suzuki reaction in context of corannulene, see: a) H. A. Wegner, L. T. Scott, A. de Meijere, *J. Org. Chem*. **2003**, *68*, 883-887; b) E. A. Jackson, B. D. Steinberg, M. Bancu, A. Wakamiya, L. T. Scott, *J. Am. Chem. Soc.* **2007**, *129*, 484-485; c) M. N. Eliseeva, L. T. Scott, *J. Am. Chem. Soc.* **2012**, *134*, 15169-15172; d) S. D. Ros, A. Linden, K. K. Baldridge, J. S. Siegel, *Org. Chem. Front.* **2015**, *2*, 626-633; e) W. B. Fellows, A. Rice, D. E. Williams, E. A. Dolgopolova, A. K. Vannucci, P. J. Pellechia, M. D. Smith, J. A. Krause, N. B. Shustova, *Angew. Chem. Int. Ed.* **2016**, *128*, 2235-2239; f) M. A. Rice, W. B. Fellows, E. A. Dolgopolova, A. B. Greytak, A. K. Vannucci, M. D. Smith, S. G. Karakalos, J. A. Kruase, S. M. Avdoshenko, A. A. Popov, N. B. Shustova, *Angew. Chem. Int. Ed.* **2017**, *129*, 4596-4600.

[21] CCDC 2005826 contains the crystallographic data for compound **5**. This data can be obtained free of charge from the Cambridge Crystallographic Data Centre.

[22] For selected examples of negatively curved systems, see: a) K. Kawasumi, Q. Zhang, Y. Segawa, L. T. Scott, K. Itami, *Nat. Chem.* **2013**, *5*, 739-744; b) C.-N. Feng, M.-Y. Kuo, Y.-T. Wu, *Angew. Chem. Int. Ed.* **2013**, *52*, 7791-7794; *Angew. Chem.* **2013**, *125*, 7945-7948; c) K. Y. Cheung, X. Xu, Q. Miao, *J. Am. Chem. Soc.* **2015**, *137*, 3910-3914; d) K. Kato, Y. Segawa, L. T. Scott, K. Itami, *Chem. Asian J.* **2015**, *10*, 1635-1639; e) K. Y. Cheung, C. K. Chan, Z. Liu, Q. Miao, *Angew. Chem. Int. Ed.* **2017**, *56*, 9003-9007; *Angew. Chem.* **2017**, *129*, 9131-9135; f) J. M. Fernández-García, P. J. Evans, S. Medina Rivero, I. Fernández, D. García-Fresnadillo, J. Perles, J. Casado, N. Martín, *J. Am. Chem. Soc.* **2018**, *140*, 17188-17196; g) I. R. Márquez, N. Fuentes, C. M. Cruz, V. Puente-Muñoz, L. Sotorrios, M. L. Marcos, D. Choquesillo-Lazarte, B. Biel, L. Crovetto, E. Gómez-Bengoa, M. T. González, R. Martin, J. M. Cuerva, A. G. Campaña, *Chem. Sci.*, **2017**, *8*, 1068-1074; h) C. M. Cruz, I. R. Márquez, I. F. A. Mariz, V. Blanco, C. Sánchez-Sánchez, J. M. Sobrado, J. A. Martín-Gago, J. M. Cuerva, E. Maçôas, A. G. Campaña, *Chem. Sci.* **2018**, *9*, 3917-3924; i) C. M. Cruz, S. Castro-Fernández, E. Maçôas, J. M. Cuerva, A. G. Campaña, *Angew. Chem. Int. Ed.* **2018**, *57*, 14782-14786; *Angew. Chem.* **2018**, *130*, 14998-15002; j) S. H. Pun, C. K. Chan, J. Luo, Z. Liu, Q. Miao, *Angew. Chem. Int. Ed.* **2018**, *57*, 1581-1586; *Angew. Chem.* **2018**, *130*, 1597-1602; k) K. Kawai, K. Kato, L. Peng, Y. Segawa, L. T. Scott, I. K. Itami, *Org. Lett.* **2018**, *20*, 1932-1935; l) S. H. Pun, Y. Wang, M. Chu, C. K. Chan, Y. Li, Z. Liu, Q. Miao, *J. Am. Chem. Soc.* **2019**, *141*, 9680-9686; m) C. M. Cruz, I. R. Márquez, S. Castro-Fernández, J. M. Cuerva, E. Maçôas, A. G. Campaña, *Angew. Chem. Int. Ed.* **2019**, *58*, 8068-8072; *Angew. Chem.* **2019**, *131*, 8152-8156.

[23] For a monkey saddle hydrocarbon, see: T. Kirschbaum, F. Rominger, M. Mastalerz, *Angew. Chem. Int. Ed.* **2020**, *59*, 270-274 *Angew. Chem.* **2020**, *132*, 276-280.

[24] The reported structures were optimized at DFT level using the ωB97X-D functional in conjunction with the Def2SVP. The thermal corrections were combined with single point energies obtained at ωB97X-D/Def2TZVPP level, and the solvation effect was taken into account by calculating single point energies for structures optimized in gas-phase using the SMD model. For further details about the applied computational methodology, see ESI-I.

[25] For a discussion on electron affinity of corannulene nucleus, see: A. Haupt, D. Lentz, *Chem. Eur. J.* **2019**, *25*, 3440-3454.

[26] a) W. Matsuoka, H. Ito, K. Itami, *Angew. Chem. Int. Ed.* **2017**, *56*, 12224-12228; *Angew. Chem.* **2017**, *129*, 12392-12396; b) K. Kato, Y. Segawa, K. Itami, *Can. J. Chem*. **2017**, *95*, 329-333.

[27] G. A. Heath, J. E. McGrady, R. L. Martin, *J. Chem. Soc., Chem. Commun.* **1992**, 1272-1274.

Entry for the Table of Contents

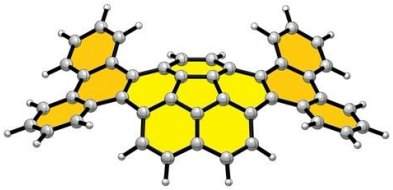

Mechanochemistry is demonstrated to be an effective and sustainable synthetic tool in the preparation of curved π-materials with high electron affinity and a highly reversible nature of the electron transfer process.